Local order in quenched states of simple atomic substances

Frank H. Stillinger and Randall A. LaViolette
AT&T Bell Laboratories, Murray Hill, New Jersey 07974-2070
(Received 30 May 1986)

In any fluid or solid condensed phase, instantaneous atomic positions can be resolved into a combination of inherent packing and of vibrational deformation components. In principle the latter can be removed by quenching the system by (mass-weighted) steepest descent on the potential-energy hypersurface. Inherent structures generated this way for a noble-gas model potential have been structurally analyzed, starting both from homogeneous liquid and from heterogeneous crystal-plus-liquid states. Quenched configurations from the homogeneous liquid show that the icosahedral mode of atom coordination is rare; instead, the more appropriate description of inherent structural disorder for the model appears to be variation of coordination number from its most probable value 12. In the case of heterogeneous systems, steepest-descent quenching induces a substantial tendency toward epitaxial crystal growth, incorporating point defects and stacking faults. Nevertheless, mechanically stable packings with side-by-side coexistence of crystalline and amorphous regions still can arise, with energy suggesting that the bonding between the two types of domains is weak.

I. INTRODUCTION

The distinct condensed phases crystal, liquid, and amorphous solid differ markedly in appearance and in measurable properties. Yet for any given substance a common set of interactions at the atomic or molecular level underlies all of these phases. This paper has as its aim the exploration of that underlying unity, using molecular-dynamics computer simulation to examine quenches (mechanically stable particle packings) that relate respectively to the various condensed phases of a simple model atomic substance.

Crystalline periodic order permits profound conceptual insights and simplifications in solid-state theory.[1] By contrast, noncrystalline liquid and solid phases present theory with a complicating and bewildering array of structural and kinetic characteristics.[2,3] Questions continue to arise about how best to describe and to classify the nonrepeating arrangements of atoms in these amorphous states, and how to understand their relation to periodic crystalline order.[4,5] Our approach has utilized a steepest-descent construction on the potential-energy hypersurface that uniquely maps any atomic configuration onto a nearby potential-energy minimum.[6,7] The resulting particle packings, prepared from several distinct initial states, have been geometrically analyzed in ways selected to help clarify some of the above issues.

Let $\mathbf{r}_1,\mathbf{r}_2,\ldots,\mathbf{r}_N$ be atomic positions, and suppose that $\Phi(\mathbf{r}_1,\mathbf{r}_2,\ldots,\mathbf{r}_N)$ represents the potential of interaction. Starting with any initial ($s=0$) configuration of atoms, the coupled steepest descent equations

$$d\mathbf{r}_j(s)/ds = -\nabla_j\Phi(\mathbf{r}_1,\mathbf{r}_2,\ldots,\mathbf{r}_N) \tag{1.1}$$

have a solution which converges in the $s\rightarrow+\infty$ limit to the relevant Φ minimum. All starting configurations which converge to a specific minimum (atom packing) define a connected "basin" surrounding that minimum. By this means, any system configuration can be uniquely resolved into the relevant packing geometry, plus a "vibrational" distortion that has displaced the system from the basin minimum. This formal separation procedure is valid regardless of the phase of matter involved or whether thermal equilibrium obtains.

When N is large the number of distinguishable Φ minima (those not merely related by permutation of identical atoms) rises exponentially with N.[8,9] The vast majority of these are relatively high in Φ and are structurally amorphous. These are the packings typically encountered upon applying the steepest-descent mapping (1.1) to the liquid[6] and to the amorphous-solid states.[7] The most nearly perfect crystal supplies the absolute Φ minimum; this and the slightly higher, slightly-defective-crystal minima compose the sparse low-potential tail of the full distribution of minima arrayed by depth. In the event that the initial configuration came from a state with a crystal-liquid interface, the packing encountered normally would exhibit side-by-side coexistence of regular crystalline and irregular amorphous regions. The present study includes each of these cases.

The specific model examined in this paper describes the heavier noble gases (Ne, Ar, Kr, Xe) reasonably well. It assumes that Φ is additively composed of central pair interactions:

$$\Phi(\mathbf{r}_1,\mathbf{r}_2,\ldots,\mathbf{r}_N)=\sum_{\substack{i,j=1\\ i<j}}^{N} v(r_{ij})\ . \tag{1.2}$$

In dimensionless units that are natural for the problem in hand, v has the following form:

$$v(r)=\begin{cases} A(r^{-12}-r^{-5})\exp[(r-a)^{-1}], & 0<r<a \\ 0, & a\le r\ , \end{cases} \tag{1.3}$$

where

$$\begin{aligned} A &= 6.767\,441\,448\ , \\ a &= 2.464\,918\,193\ . \end{aligned} \tag{1.4}$$

This is a somewhat foreshortened version of the reduced Lennard-Jones (LJ) interaction

$$v_{\mathrm{LJ}}(r)=4(r^{-12}-r^{-6}),\quad 0<r\ , \tag{1.5}$$

and as a result of the specific values chosen for A and a the following three attributes are shared both by v and by v_{LJ}:

$$\begin{aligned} &v(1)=v_{\mathrm{LJ}}(1)=0\ ,\\ &v(2^{1/6})=v_{\mathrm{LJ}}(2^{1/6})=-1\ ,\\ &v'(2^{1/6})=v'_{\mathrm{LJ}}(2^{1/6})=0\ . \end{aligned} \tag{1.6}$$

The function v is superior to v_{LJ} in describing the heavier noble gases in that it correctly leads to the face-centered-cubic crystal as its absolute Φ minimum, while v_{LJ} leads to the hexagonal close-packed structure.[10]

The fact that v vanishes identically beyond distance a is advantageous for molecular dynamics applications. Furthermore all derivatives of v are continuous at this point, which is important in achieving high-accuracy numerical solutions to Newton's equations of motion.

In Sec. II we examine short-range order in a collection of amorphous packings that were prepared [via Eqs. (1.1)] from the thermodynamically stable liquid in a molecular dynamics simulation. Primary interest concerns $g_q^{(2)}(r)$, the pair-correlation function for these packings. This function is sufficiently structured that it naturally suggests a distance criterion for the purpose of identifying the "nearest neighbors" of any given particle. As a consequence we have an easily implemented alternative to construction of nearest-neighbor polyhedra surrounding each atom.[11] Subsequently particles can be classified according to the number of nearest neighbors they possess, and we have calculated concentrations of particles so classified.

Once nearest-neighbor sets have been identified for each particle, one can ask how those neighbors are arranged spatially. It has been suggested[12–14] that a basic structural ingredient in strongly supercooled liquids and amorphous solids is icosahedral coordination. Consequently a geometric test is formulated and applied in Sec. III to identify those 12-coordinate particles in our amorphous packings that display icosahedral character.

Particles possessing different numbers of nearest neighbors may be regarded formally as distinct species, and so the entire system amounts to a multicomponent mixture of these species. Separate pair-correlation functions can then be defined to describe the spatial distribution of these species. For example, $g(r\mid 11,13)$ would represent the pair distribution (suitably normalized) for particles respectively with 11 and with 13 nearest neighbors. Section IV presents results for these $g(r\mid\mu,\nu)$ in our noble-gas-model amorphous packings.

Section V takes up the issue of spatially inhomogeneous packings. Specific examples have been formed with 1008 atoms under periodic boundary conditions with amorphous portions in contact with the (111) surface of an fcc crystalline slab. These structures show that periodic order tends strongly to propagate into the amorphous region with slow spatial decay.

The final Sec. VI presents some ancillary calculations, and considers a few implications of this study for future work.

II. AMORPHOUS PACKING CORRELATION FUNCTION

The model defined by Eqs. (1.2)–(1.4) above exhibits a perfect fcc crystal at vanishing temperature and pressure[15] with reduced density

$$\rho=1.066\,27\ , \tag{2.1}$$

and reduced binding energy per particle

$$\Phi/N=-7.162\,077\ . \tag{2.2}$$

The melting point temperature T_m at the "natural" density (2.1) has been determined by molecular dynamics simulation to be[16]

$$T_m\cong 2.40\ . \tag{2.3}$$

For the present study a new series of molecular dynamics calculations with periodic boundary conditions has been carried out at the same density (2.1). Systems containing either 256 or 1008 particles have been examined.

Using the smaller system size, a well-equilibrated hot liquid at reduced temperature 6.20 has been prepared. During the constant-energy time evolution of this liquid, a set of 11 configurations was selected, separated by equal reduced time intervals $\Delta t=0.012$. Self-diffusion is sufficiently rapid at this temperature and density that these 11 configurations can be regarded as substantially independent. Each of them in turn served as initial condition for numerical integration of the steepest-descent equations

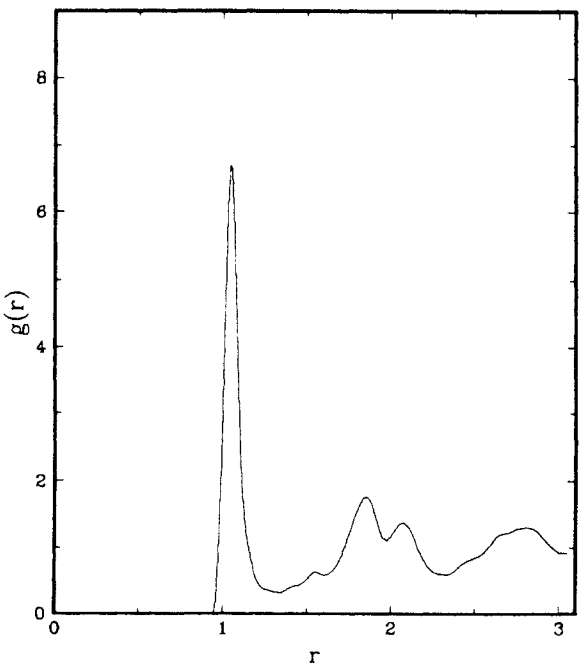

FIG. 1. Particle pair-correlation function $g_q^{(2)}(r)$ for 11 amorphous packings prepared by steepest-descent mapping from the liquid at $T=6.20$.

(1.1), resulting in a corresponding set of 11 particle packings. These packings (for which all forces vanished) were verified to be valid local minima by diagonalizing the Hessian matrix for Φ and observing that all but a vanishing triad of its eigenvalues were positive. The potential energies of all of these packings were distinct, and each was substantially higher than the absolute minimum ($\Phi = -1833.492$) indicated in Eq. (2.2). The mean depth of these amorphous packings was found to be

$$\langle \Phi \rangle = -1651.142 , \tag{2.4}$$

which is representative of the region of the density maximum in the full distribution of minima arrayed by depth.[16]

The pair-correlation function $g_q^{(2)}(r)$ has been evaluated as an average over the 11 packings. It appears in Fig. 1. Its form is virtually identical (within statistical uncertainty) to those previously found for the same model but with different initial liquid temperatures,[15] and this implies that the common $g_q^{(2)}(r)$ reveals an inherent packing structure for the liquid phase.

The function shown in Fig. 1 is much more structured than the conventional pair correlation functions $g^{(2)}(r)$ for the liquid phase, owing to removal of vibrational deformation by the steepest-descent mapping (1.1). In particular, the first peak and subsequent minimum are much better developed, and this suggests a straightforward and obvious definition of "nearest neighbors" in terms of the position of that minimum,

$$r_m = 1.35 . \tag{2.5}$$

Thus, any and all particles lying closer to a given particle than r_m are to be regarded as its nearest neighbors. The first- and second-neighbor shells in the fcc lattice at this density occur at distances 1.0987 and 1.5538, respectively, so the criterion correctly assigns precisely 12 neighbors to each particle in the crystal.

Table I shows the various fractions of particles in the 11 amorphous packings with different coordination numbers. None of the $2816 (= 11 \times 256)$ cases showed less than 9 or more than 15 nearest neighbors. We see that even after disruption of the fcc structure to form the amorphous packings, 12 continues to be the most probable coordination number. Nevertheless deviations from this value are frequent.

TABLE I. Coordination number distribution for amorphous packings. Obtained from 11 amorphous packings of 256 particles at reduced density 1.066 27, with periodic boundary conditions. Nearest-neighbor (coordination) number n is defined by Eq. (2.5).

n	No. of cases	Fraction
9	3	0.001 065
10	59	0.020 952
11	593	0.210 582
12	1465	0.520 241
13	607	0.215 554
14	86	0.030 540
15	3	0.001 065

To put these last results in context, it is worth noting how the smallest elements of stable packing disorder, namely point defects, affect particle coordination numbers.

A monovacancy can be formed by removing a single particle from the fcc crystal while leaving the box size unchanged. The potential energy of the resulting 255 particle system at its (relaxed) mechanical stability point is

$$\Phi(\text{monovacancy}) = -1819.237 . \tag{2.6}$$

Distortion around the vacant site is minimal. The 12 particles that were nearest neighbors of the now-missing particle only have 11 neighbors, while all other particles continue to have 12.

The lowest potential energy configuration for an fcc crystal with an extra particle (i.e., total of 257) exhibits a "split interstitial," that is, a pair of particles symmetrically flanking a nominal crystal lattice site. This split interstitial in the present model is always aligned along one of the principle cube directions. The potential energy of such a 257-particle packing in the same volume as before is the following:

$$\Phi(\text{split interstitial}) = -1810.939 . \tag{2.7}$$

Now one finds that two particles (the split interstitial pair) have 10 neighbors by the criterion using Eq. (2.5), none have 11, six have 13 neighbors, and all the rest remain 12 coordinate.

A large fcc crystal containing several vacancies and split interstitials that are all well separated from each other would have occurrences of non-12 coordinations that are additive over the defects. However, closely clustered defects would violate this additivity, the divacancy providing a simple illustration. In the interests ultimately of explaining results in Table I, we mention that a formally exact procedure exists for classifying any arbitrary packing as a point-defect-containing crystalline medium.[9]

III. TEST FOR ICOSAHEDRAL COORDINATION

Twelve spherical particles can be symmetrically packed around a thirteenth in three distinct ways as shown in Fig. 2.[12] The face-centered cubic (fcc) and the hexagonal close-packed (hcp) options can be used to build up strain-free packings of arbitrarily large numbers of particles. The icosahedral option cannot; outward growth of a central icosahedral seed using essentially the same mode of coordination soon produces geometric frustration and strain. Nevertheless, it has been proposed that icosahedral coordination is a basic structural motif in amorphous states of atomic substances,[12–14] and so it is natural to wonder if the present model conforms to this idea. Consequently we have examined the collection of 11 amorphous packings of 256 particles for the presence of intact icosahedra, an issue that cannot be resolved merely by examining $g^{(2)}$ or $g_q^{(2)}$.

Our testing algorithm is based upon the existence of square faces in the fcc and hcp coordination polyhedra, while none are present in the icosahedron (see Fig. 2).

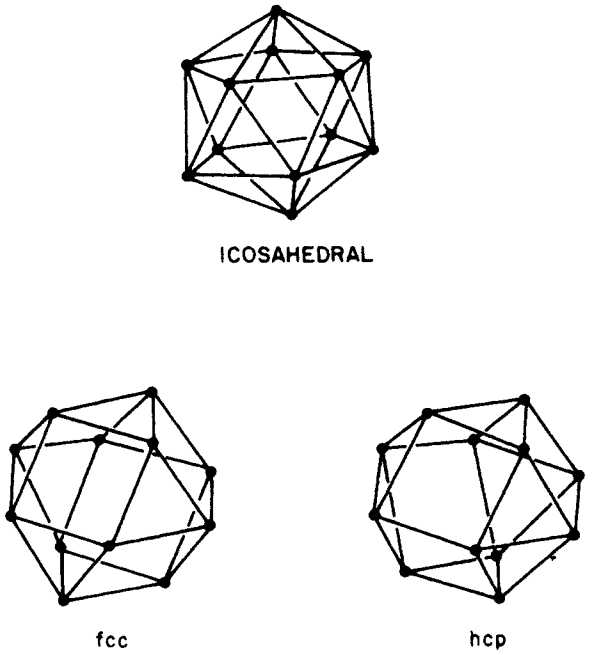

FIG. 2. Symmetrical coordination modes for 12 particles (shown as vertices) around a thirteenth.

The pair correlation function $g_q^{(2)}(r)$ in Fig. 1 shows that radial distances to nearest neighbors, while not all identical, nevertheless are rather narrowly distributed around the most probable value $r=1.05$. Focusing attention just on the qualifying 12-coordinate particles, the set of 66 scalar distances are calculated for all pairs of particles in each of these coordination spheres. Table II shows the set of distances to be expected if the radius were exactly 1.05, and if each of the three coordination geometries were present in completely undeformed fashion. Square faces for the fcc and hcp cases contribute distances equal to 1.4849 in Table II.

Taking due account of nearest-neighbor bond-length fluctuations in $g_q^{(2)}(r)$, it seems reasonable to suppose that an icosahedral coordination shell will be devoid of pair distances in the interval

$$1.20 < r < 1.55 \ . \tag{3.1}$$

Table II shows that the other two twelvefold coordination modes violate this criterion.

TABLE II. Ideal coordination shell distances for each of the three cases shown in Fig. 2. The coordinate-shell radius is assumed to be 1.0500 for all three cases. Integers in parentheses give the number of occurrences of each distance.

fcc	hcp	Icosahedral
1.0500 (24)	1.0500 (24)	1.1040 (30)
1.4849 (12)	1.4849 (12)	1.7864 (30)
1.8187 (24)	1.7146 (3)	2.1000 (6)
2.1000 (6)	1.8187 (18)	
	2.0106 (6)	
	2.1000 (3)	

The 1465 examples of twelvefold coordination listed in Table I for the amorphous packings were all examined in turn to see if they satisfied this geometric criterion. In fact none did. Only one of the 1465 had as few as one violation, i.e., one of the 66 shell distances in the sensitive range (3.1); careful examination showed that this one case could be viewed as a distorted icosahedron. Increasing numbers of examples from the set of 1465 exhibited increasing numbers of distance violations. Perhaps these might also be regarded as distorted icosahedra, but it should be kept in mind that even the perfect fcc and hcp geometries formally could be viewed as grossly distorted icosahedra.

The conclusion seems to be that amorphous packings for the noble-gas model under consideration do not have icosahedral coordination as an important structural element. Icosahedra are infrequent, distorted, and only inadvertent inclusions in a random structure that relies more heavily on the other two types of twelvefold coordination. Deviations of the coordination number from 12 as in Table I seem to be a much more important ingredient in producing amorphous structures for the present model.

IV. RESOLVED PAIR CORRELATIONS

Further insights into the structure of the amorphous deposits emerge from resolution of the pair-correlation function $g_q^{(2)}(r)$ into separate components $g(r \mid \mu,\nu)$ which refer to the spatial distributions of particles distinguished by their coordination numbers (μ and ν). This kind of analysis has been useful before in studying two-dimensional many-body systems.[17] Specifically,

$$N(N-1)g_q^{(2)}(r)=\sum_{\mu,\nu}\langle N_\mu(N_\nu-\delta_{\mu\nu})\rangle g(r \mid \mu,\nu) \ , \tag{4.1}$$

where N_μ is the number of particles with μ nearest neighbors as defined in the preceding Sec. III, and N is the total number of particles (256 for the present case):

$$N=\sum_\mu N_\mu \ . \tag{4.2}$$

The angular brackets in Eq. (4.1) denote an average over the available collection of packings. The idea underlying Eq. (4.1) is that the different groups of particles with different coordination numbers can be treated as distinct species mixed together in the system, and that the $g(r \mid \mu,\nu)$ then are simply the pair-correlation functions for distinct pair types in this mixture. Obviously we have the symmetry condition

$$g(r \mid \mu,\nu)=g(r \mid \nu,\mu) \ . \tag{4.3}$$

If our earlier conclusion for the noble-gas model is correct that coordination number deviations from 12 are the principal type of defect present in the amorphous packings, then $g(r \mid 12,12)$ should display the most obvious order of all of the $g(r \mid \mu,\nu)$. Furthermore, the short-range order revealed by $g(r \mid 12,12)$ should closely resemble that for close-packed crystals.

Using the 11 amorphous packings of 256 atoms, we have evaluated the six independent functions $g(r \mid \mu,\nu)$

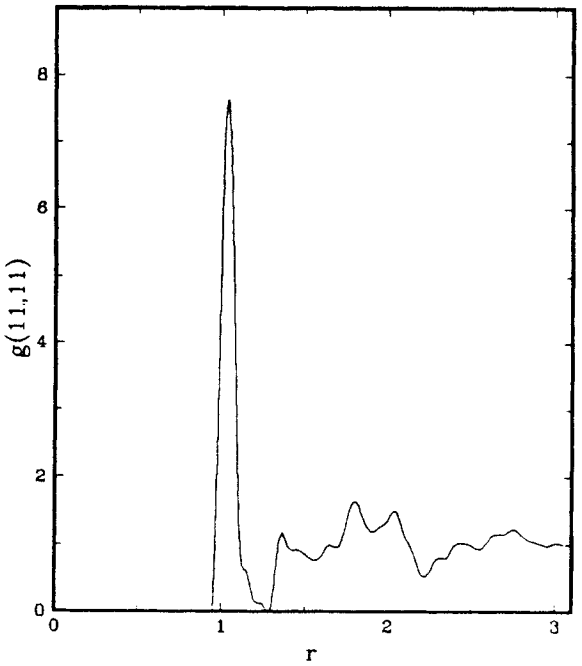

FIG. 3. Pair-correlation function in the random packings for particles both of which have 11 nearest neighbors.

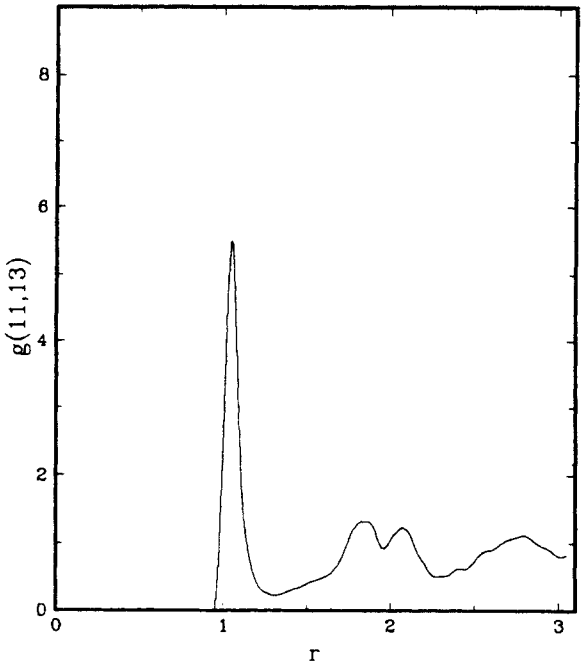

FIG. 5. Pair-correlation function for the random packings where one particle has 11 nearest neighbors, the other has 13.

for μ and ν equal to 11, 12, and 13. As Table I indicates, too few particles appeared with other coordination numbers to permit statistically significant determination of the other $g(r \mid \mu,\nu)$. Our results are presented in Figs. 3–8.

Out of the six functions shown, $g(r \mid 12,12)$ does indeed seem to be indicative of the most regular short-range order. This conclusion is based on the following observations.

(1) $g(r \mid 12,12)$ has the highest first-neighbor peak.

(2) Considering peaks beyond that for nearest neighbors, $g(r \mid 12,12)$ has the most prominent (its third peak, with value exceeding 2).

(3) The first four peaks of $g(r \mid 12,12)$ occur at distances roughly in the ratios 1, $2^{1/2}$, $3^{1/2}$, 2 that appear as successive coordination shell positions in the fcc structure (and also as some of the hcp successive shells).

In contrast to $g(r \mid 12,12)$, the five other functions shown all indicate structural disruption in one way or

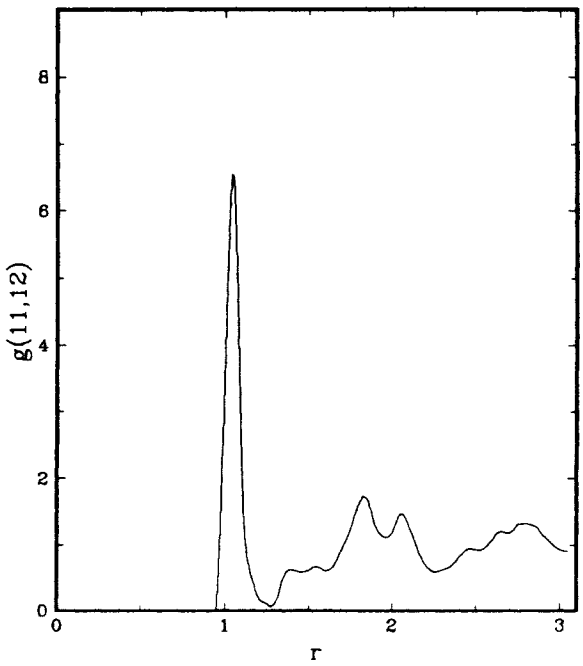

FIG. 4. Pair-correlation function in the random packings where one particle has 11 nearest neighbors, the other has 12.

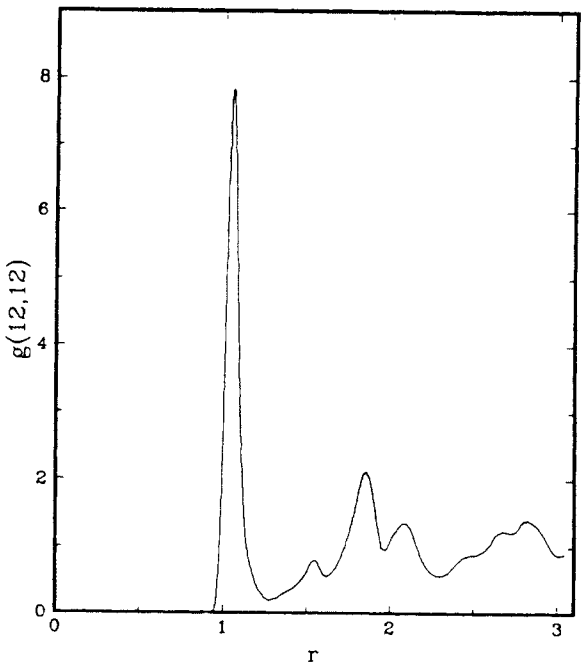

FIG. 6. Pair-correlation function in the random packings for particles both of which have 12 nearest neighbors.

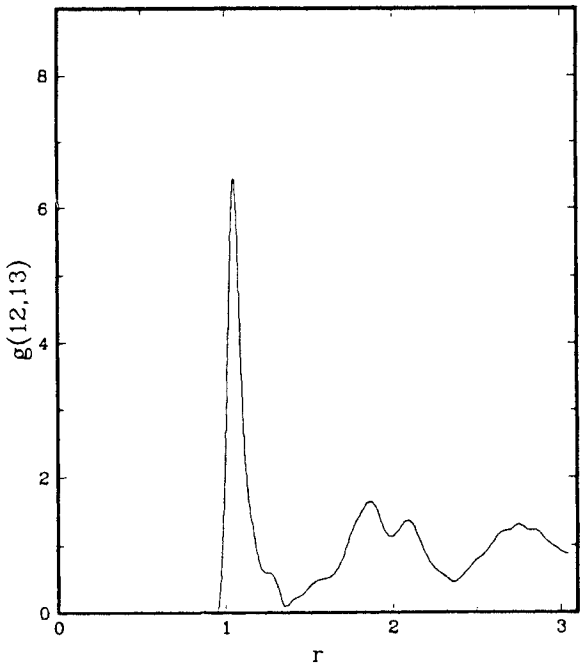

FIG. 7. Pair-correlation function in the random packings where one particle has 12 nearest neighbors, the other has 13.

another. For example, $g(r \mid 11,13)$ seems to show the same features as $g(r \mid 12,12)$ but in a much diminished way. In the case of $g(r \mid 12,13)$ the "extra" particle shows up as a small shoulder on the large-r side of the first peak, and apparently perturbs local order at yet larger r; this is even more evident for $g(r \mid 13,13)$.

The "correctly coordinated" particles with 12 nearest neighbors are randomly dispersed throughout the amorphous packings. They are sufficiently high in concentration to be above a critical percolation threshold: Connected pathways across the system should exist passing from one twelvefold coordinated particle to one of its neighbors which is also twelvefold coordinated (on average there are 6.5) to a third twelvefold coordinated particle, etc. Indeed, the concentration of correctly coordinated particles constitutes a relevant order parameter, and it would be interesting eventually to determine how packing energies and entropies depend on this order parameter.

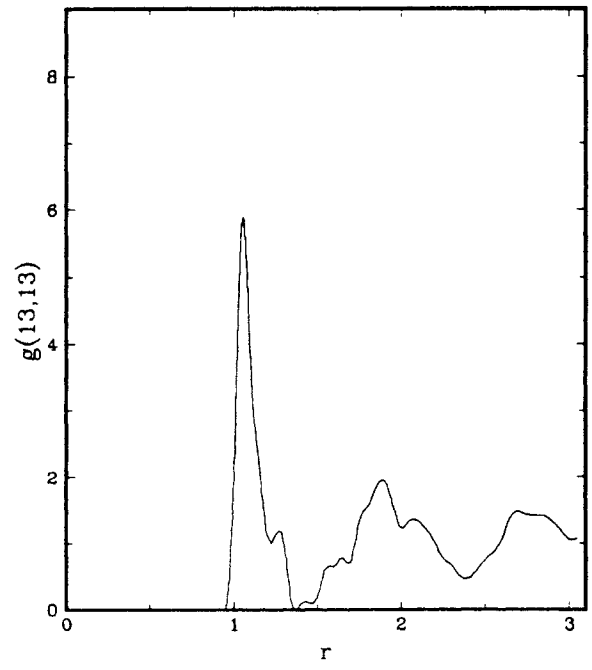

FIG. 8. Pair-correlation function in the random packings for particles both of which have 13 nearest neighbors.

V. INHOMOGENEOUS PACKINGS

While application of steepest-descent mapping (1.1) to configurations in the liquid can be used to generate homogeneous amorphous packings, a different procedure is required to produce inhomogeneous packings. These latter, by definition, display a substantial spatial variation in the coordination number order parameter, the local concentrations of twelvefold coordinated particles. For this purpose a set of 1008-particle calculations was carried out using the same density (2.1) and periodic boundary conditions as before. Now, however, the system resides in a rectangular box with dimensions

$$L_x = 7.69096, \quad L_y = 7.61208, \quad L_z = 16.14766 . \tag{5.1}$$

The perfect fcc crystal fits into this box without strain, oriented so that 18 close-packed layers (each containing 56 particles) stack perpendicular to the z axis.

In order to search for inhomogeneous packings, a contiguous subset (slab) of the 18 close-packed layers was held fixed while the remaining particles were subjected to high-temperature ($T > 5$) molecular dynamics for a period sufficient to disrupt their periodic order. The resulting configuration was then used as the starting point for a steepest-descent mapping Eq. (1.1) that involved moving *all* 1008 particles to the relevant Φ minimum. Trials of this sort were attempted in which 4, 9, and 14 contiguous planes were held fixed.

In those cases with 9 or 14 of the close-packed (111) planes initially fixed, and occasionally with 4 planes fixed, we found that the system recrystallized during the steepest descent mapping. This is not to say that the perfect fcc crystal reappeared, but the crystalline structure that spontaneously formed contained stacking faults (in all cases) and point defects (usually). Figure 9 shows a side view of one of these defective crystals. Evidently epitaxial regrowth has easily overcome the disorder introduced in the relatively narrow space between the initially constrained layers.

When only four layers are fixed there is a reasonable chance that an inhomogeneous packing will emerge from the steepest-descent mapping. Figure 10 shows one of these, whose potential energy,

$$\Phi = -6449.7456 , \tag{5.2}$$

lies significantly higher than the average we find for fully amorphous packings of the 1008 particles ($\Phi \cong -6480$). This indicates that the crystalline-amorphous interface is energetically unfavorable, and may be evidence that the

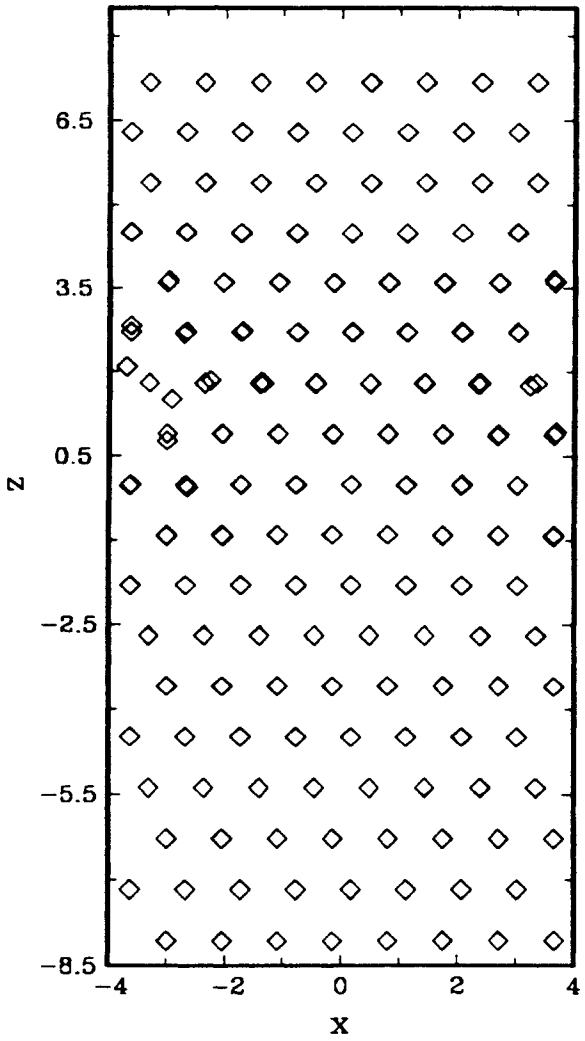

FIG. 9. Defective crystal composed of 1008 particles, with potential energy $\Phi = -7181.8548$. This structure was formed from an initial state with four contiguous close-packed layers held fixed, the remainder of the system strongly disordered.

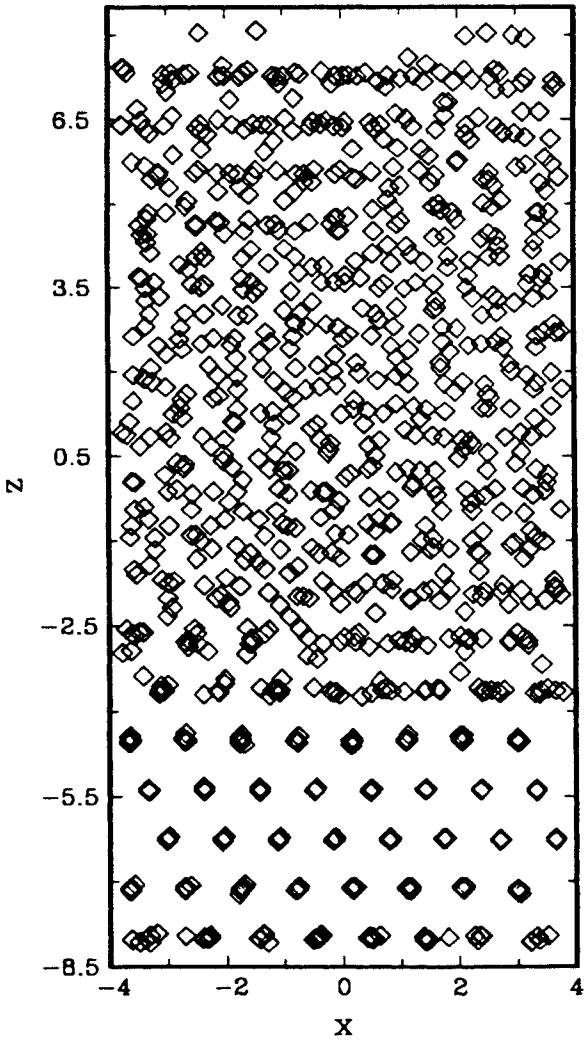

FIG. 10. Inhomogeneous packing of 1008 particles, with potential energy $\Phi = -6449.7456$. Four contiguous close-packed layers near the bottom of the system were initially held fixed while the remainder of the system was strongly disordered.

bond between the two regions is mechanically weak.

Although it is desirable to check the 1008-particle packings for stability as before with 256 particles, the Hessian matrix is too large to diagonalize conveniently. Fortunately another option exists. The inhomogeneous packing in Fig. 10 was used as the initial configuration (with small momenta assigned to particles) for a long, very-low-temperature molecular dynamics run. During this run it was observed that all particles stably executed only small vibrations around their starting points. If the steepest-descent mapping had falsely converged onto a saddle point, the molecular dynamics would have revealed positional instability as the system rolled off that saddle point toward one of its flanking minima.

Figure 10 shows that the initially-constrained crystalline slab (the four layers in the range $-7.5 \leq z \leq -4.5$) induces density stratification in that portion of the amorphous region nearest its surfaces. Analysis of particle positions discerns that at least four density maxima (with respect to direction z) have formed during the steepest descent, with amplitudes that diminish with distance from the slab.

Two types of particle sites exist on the exposed (111) surface of a crystalline slab that could be used for continued growth of the crystal. Only one of these types would be used to extend the fcc lattice, while the other leads to stacking in the hcp mode. The reason for the existence and stability of inhomogeneous packings is that both types of sites have simultaneously been used in formation of the first new layer. This creates gaps which disrupt the positional order of subsequent layers. As these latter settle into place the geometric disorder increases with distance from the ordered slab substrate.

The site degeneracy on the (111) surface does not exist for the (100) surface. Consequently we believe that under our boundary conditions even larger systems would be required in order to create inhomogeneous packings with an amorphous position in contact with this crystal surface.

There would probably be a greater tendency for epitaxial crystal growth in this latter case, and the crystalline-amorphous interface would have to be stabilized by a new mechanism. It should be mentioned in passing that Abraham, Tsai, and Pound have reported[18] Monte Carlo construction of a (100)-amorphous interface with truncated Lennard-Jones interactions; however, the system size and boundary conditions were different from those used here, and mechanically stable structures were not sought in that study.

VI. DISCUSSION

The scarcity of icosahedral coordination geometry in amorphous packings for our model, even as twelvefold coordination in general is very frequent, constitutes one of the major conclusions in this study. Although this result is primarily based on our 256-particle calculations (Sec. III), we have also found confirmation from a few calculations with 1008 particles. The larger systems placed into homogeneous amorphous packings have potential energies per particle and short-range orders in close agreement with those found for the smaller systems, and likewise they show only rare (about 1 in 10^3 particles) occurrences of icosahedral coordination.

But while the icosahedral mode of packing may be rare within the interior of an amorphous deposit, it may be present in considerably higher concentration near a free surface of such deposits. The presence of that free surface would at least partially eliminate the built-in strain that accompanies the three-dimensional outward propagation of icosahedral packing. Future studies might profitably compare the coordination statistics of free surface and of interior positions of amorphous packings.

We stress that our failure to observe substantial numbers of icosahedra is restricted only to the one model interaction given by Eqs. (1.2)–(1.4), and should not be taken as evidence against such behavior for significantly different interactions. No doubt there will be choices of nonadditive interactions and/or of multicomponent systems that have far stronger tendency to incorporate icosahedral packing within the interior of their amorphous deposits.

It is obvious that changing the number N of particles strongly influences the number of potential-energy minima (packings) available to the system. In the large-N limit, the constant-density number of minima $\Omega(N)$ is expected to show the asymptotic form[8,9]

$$\Omega(N) \sim N! \exp(\nu N) , \tag{6.1}$$

where the factorial accounts for permutations of particles. The positive constant ν will depend on density and the form of interaction, but for simple atomic substances it appears to lie in the range 0.1–0.5.[9,19]

Subtle effects on the distribution of potential minima can occur for relatively small N values, and future investigations would be well advised to take them into account. The case of $N=243$ serves to illustrate this point for our model, Eqs. (1.2)–(1.4). Using the same cubical box size ($L=6.21524$) as for 256 particles at density (2.1), the absolute Φ minimum is

$$\Phi(243) = -1686.907 , \tag{6.2}$$

corresponding structurally to a compact 13-vacancy in what is otherwise a defect-free fcc crystal. That is, the lowest energy is obtained by removing from the perfect $N=256$ crystal a particle and its surrounding 12 nearest neighbors. Higher lying minima for $N=243$ have also been investigated, by using the steepest-descent procedure from a collection of high-temperature fluid configurations. We have never been able to produce an amorphous packing of 243 particles by this procedure. Instead the resulting packings always consist of a dispersed arrangement of the 13 vacancies in the fcc lattice.

The reason for this last peculiarity seems clear. The number of distinct ways that 13 vacancies can be distributed over 256 crystal sites is given by the elementary combinatorial expression

$$\frac{256!}{13!243!} = \exp(243\nu), \quad \nu = 0.20257\ldots . \tag{6.3}$$

The exponential format for writing this number is useful in light of expression (6.1). Since the resulting ν value falls in the expected range for *all* distinct packings, it seems clear that vacancy-containing crystalline packings in this case are so numerous that their basins exhaust virtually the entire configuration space. Nothing is left for amorphous packings.

Unfortunately it is not yet entirely clear what combinations of box sizes and of particle numbers N will produce this situation. However when it does exist it is likely to influence the rate of crystal nucleation from the melt. The system is always close to some (defective) crystalline structure, needing only to travel downward within a basin to achieve such a packing, and does not need to "undo" an everywhere amorphous arrangement of particles. It is possible that this phenomenon underlies the N-dependent nucleation rates that have been reported by Honeycutt and Andersen for molecular dynamics simulations with a truncated Lennard-Jones pair potential.[20]

[1] C. Kittel, *Introduction to Solid State Physics*, 5th ed. (Wiley, New York, 1976).

[2] J. P. Hansen and I. R. McDonald, *Theory of Simple Liquids* (Academic, New York, 1976).

[3] *The Structure of Non-Crystalline Materials*, edited by P. H. Gaskell (Taylor and Francis, London, 1977).

[4] Structure and Mobility in Molecular and Atomic Glasses, edited by J. M. O'Reilly and M. Goldstein [Ann. N.Y. Acad. Sci. 371 (1981)].

[5] J. C. Phillips, Phys. Today 35(2), 27 (1982).

[6] F. H. Stillinger and T. A. Weber, Phys. Rev. A 28, 2408 (1983).

[7] T. A. Weber and F. H. Stillinger, Phys. Rev. B 31, 1954 (1985).

[8] F. H. Stillinger and T. A. Weber, Phys. Rev. A 25, 978 (1982).

[9] F. H. Stillinger and T. A. Weber, J. Chem. Phys. 81, 5095 (1984).

[10] J. O. Hirschfelder, C. F. Curtiss, and R. B. Bird, *Molecular Theory of Gases and Liquids* (Wiley, New York, 1954), p. 1041.

[11] R. Collins, in *Phase Transitions and Critical Phenomena*, edited by C. Domb and M. S. Green (Academic, New York,

1972), Vol. 2, pp. 271–303.
[12]F. C. Frank, Proc. R. Soc. London, Ser. A **215**, 43 (1952).
[13]J. F. Sadoc, J. Non-Cryst. Solids **44**, 1 (1981).
[14]P. J. Steinhardt, D. R. Nelson, and M. Ronchetti, Phys. Rev. B **28**, 784 (1983).
[15]F. H. Stillinger and R. A. LaViolette, J. Chem. Phys. **83**, 6413 (1985).
[16]R. A. LaViolette and F. H. Stillinger, J. Chem. Phys. **83**, 4079 (1985).
[17]T. A. Weber and F. H. Stillinger, J. Chem. Phys. **74**, 4020 (1981).
[18]F. F. Abraham, N.-H. Tsai, and G. M. Pound, Surf. Sci. **78**, 181 (1978).
[19]T. A. Weber and F. H. Stillinger, J. Chem. Phys. **80**, 2742 (1984).
[20]J. D. Honeycutt and H. C. Andersen, Chem. Phys. Lett. **108**, 535 (1984); J. Phys. Chem. (to be published).